Magnetic and structural properties of the magnetic shape memory compound $Ni_2Mn_{1.48}Sb_{0.52}$

2010 J. Phys.: Condens. Matter 22 096002

(http://iopscience.iop.org/0953-8984/22/9/096002)

J. Phys.: Condens. Matter **22** (2010) 096002 (9pp) doi:10.1088/0953-8984/22/9/096002

Magnetic and structural properties of the magnetic shape memory compound $Ni_2Mn_{1.48}Sb_{0.52}$

P J Brown[1,2], A P Gandy[1], K Ishida[3], W Ito[4], R Kainuma[4], T Kanomata[5], K U Neumann[1], K Oikawa[3], B Ouladdiaf[2], A Sheikh[1] and K R A Ziebeck[1,6]

[1] Department of Physics, Loughborough University, Leicestershire LE11 3TU, UK
[2] Institut Laue-Langevin, BP 156, 38042 Grenoble, France
[3] Department of Material Science, Graduate School of Engineering, Tohoku University, 6-6-02 Aoba-yama, Sendai 980-8579, Japan
[4] Institute of Multidisciplinary Research for Advanced Materials, Tohoku University, 2-1-1 Katahira, Sendai 980-8577, Japan
[5] Faculty of Engineering, Tohoku Gakuin University, Tagajo 985-8537, Japan

Received 26 November 2009, in final form 14 January 2010
Published 10 February 2010
Online at stacks.iop.org/JPhysCM/22/096002

Abstract

Magnetization and high resolution neutron powder diffraction measurements on the magnetic shape memory compound $Ni_2Mn_{1.48}Sb_{0.52}$ have confirmed that it is ferromagnetic below 350 K and undergoes a structural phase transition at $T_M \approx 310$ K. The high temperature phase has the cubic $L2_1$ structure with $a = 5.958$ Å, with the excess manganese atoms occupying the 4(b) Sb sites. In the cubic phase above ≈310 K the manganese moments are ferromagnetically aligned. The magnetic moment at the 4(a) site is 1.57(12) μ_B and it is almost zero (0.15(9) μ_B) at the 4(b) site. The low temperature orthorhombic phase which is only fully established below 50 K has the space group *Pmma* with a cell related to the cubic one by a Bain transformation $\mathbf{a}_{orth} = (\mathbf{a}_{cub} + \mathbf{b}_{cub})/2$; $\mathbf{b}_{orth} = \mathbf{c}_{cub}$ and $\mathbf{c}_{orth} = (\mathbf{a}_{cub} - \mathbf{b}_{cub})$. The change in cell volume is ≈2.5%. The spontaneous magnetization of samples cooled in fields less than 0.5 T decreases at temperatures below T_M and at 2 K the magnetic moment per formula unit in fields up to 5.5 T is 2.01(5) μ_B. Neutron diffraction patterns obtained below ≈132 K gave evidence for a weak incommensurate magnetic modulation with propagation vector (2/3, 1/3, 0).

(Some figures in this article are in colour only in the electronic version)

1. Introduction

Ferromagnetic shape memory alloys can show magnetic field induced strains of over 5% by the rearrangement of twin variants in the martensitic phase [1]. With this mechanism the speed of shape change is not limited as it is in conventional shape memory alloys [2, 3]. These alloys are therefore potential smart materials for use in magneto-mechanical actuators etc. Up to now several candidates, all based on Ni_2MnGa [4] have been identified; but although a large strain ($|1 - c/a|$), up to ≈0.12 [5], can be obtained for a multivariant tetragonal martensite the output stress is limited to ≈4 MPa. This shortcoming may be remedied if the martensitic transformation is itself field dependent [6]. The change ΔT in the transformation temperature obtained from a variation ΔB in applied field can be estimated using the Clausius–Clapeyron relation;

$$\Delta T_M = -\left(\frac{\Delta M}{\Delta S}\right)\Delta B$$

in which ΔM and ΔS are the differences in magnetization and entropy between the austenite and martensite phases. To produce a large change in ΔT_M requires a large ΔM and small ΔS. In Ni–Mn–Ga alloys ΔM is small so that T_M varies by only ≈1.6 K in fields of 2 T [7]. Furthermore these materials tend to be brittle and the phase change essential for shape

[6] Present address: Cavendish Laboratory, Cambridge CB3 0HE, UK.

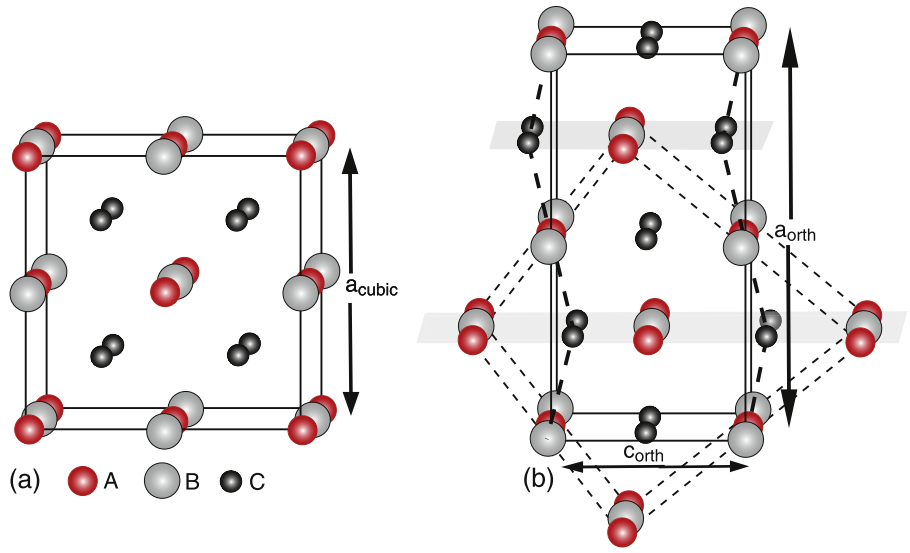

Figure 1. (a) The ideal Heusler L21 cubic structure (ABC_2), (b) the atomic displacements giving rise to the $(2\bar{2})$ orthorhombic phase.

memory behaviour occurs well below room temperature which limits their potential for application. Recently new families of ferromagnetic shape memory compounds have been reported based on the ternary series $Ni_{50}Mn_{50-x}Z_x$ (Z = In, Sn and Sb) [8, 9]. These compounds are reported to transform from the cubic Heusler parent phase, figure 1(a), to a modulated martensitic phase in a two or three step process. Studies using transmission electron microscopy and x-ray diffraction suggest that the martensitic phase of the Sn and Sb alloys has a four layered orthorhombic structure with lattice parameters $a \approx 5.9$ Å, $b \approx 2.87$ Å, $c \approx 8.4$ Å and a $(2\bar{2})$ stacking sequence. The Ni and Mn atoms were not distinguishable so that the true unit cell has $b = 5.74$ Å as shown in figure 1(b).

Magnetic field induced structural phase transitions have been reported for the Sn compounds $Ni_{50}Mn_{50-x}Z_x$ with $x = 14$ [10] and for the In compounds with $x = 16$ [6]. However magnetization measurements on the Sn compound have shown that fields up to 5.5 T have no effect on T_M and recent neutron powder diffraction measurements at 200, 230 and 250 K in fields up to 5.5 T confirm that the structure is field invariant [11]. Equivalent measurements on the related Sb compound have not yet been reported and it is to fill this gap that the current investigation of the crystallographic and magnetic structures of $Ni_2Mn_{1.48}Sb_{0.52}$ has been undertaken. Partial magnetic phase diagrams for Ni–Mn–Sb alloys based on bulk measurements have been reported [8, 12]. Sutou [8] used DSC measurements to establish the martensite (M_S, M_F) and austenite (A_S, A_F) start and finish temperatures in $Ni_2Mn_{1.48}Sb_{0.52}$. The results for the heating and cooling cycles lead to a mean transition temperature $T_M = (M_S + A_F)/2 \approx 300$ K. The same measurements established the Curie temperature as 333 K. A large positive magneto-entropy change has been observed [13] in the vicinity of the martensitic transition with a maximum value of 9.1 J T^{-1} together with a magnetic field induced shape recovery strain of ≈15 ppm in fields of up to 1.2 T.

1.1. Structural phase transition

High resolution neutron diffraction measurements have shown that a number of Heusler alloys undergoing a martensitic phase transition, transform from the cubic parent phase to an orthorhombic structure. The orthorhombic phase is based on a tetragonal cell derived from the cubic fcc cell by a Bain type transformation as shown in figure 1. The transformation between the axes of the cubic and orthorhombic cells is

$$\begin{pmatrix} \frac{n}{2} & \frac{n}{2} & 0 \\ 0 & 0 & 1 \\ \frac{1}{2} & -\frac{1}{2} & 0 \end{pmatrix}$$

where n is an integer defining the period of modulation along $[\frac{1}{2}\frac{1}{2}0]$ which gives rise to orthorhombic symmetry. For the prototype ferromagnetic shape memory alloy Ni_2MnGa $n = 7$ [14] whereas for Co_2NbSn [15] and $Ni_2Mn_{1.44}Sn_{0.56}$ [16] $n = 2$. It has been shown [17] that in Ni_2MnGa the phase transition takes place by two successive shears on {110} planes in ⟨110⟩ directions and strain in the martensitic phase is accommodated by twinning rather than by slip. The shape memory property is then due to the fixed orientation relationship between the martensitic twins and the high temperature cubic axes. In the Ni–Fe–Ga ferromagnetic shape memory system the martensitic phase has a different structure from that of Ni_2MnGa and the c/a ratio of the pseudo-tetragonal phase is greater than as opposed to less than 1. The transformation mechanism involves only one shear and the orientation relationships between the martensitic variants, which are fundamental in determining the shape memory behaviour, are different [18].

2. Experimental details

A 20 g ingot of $Ni_2Mn_{1.48}Sb_{0.52}$ was prepared by melting the appropriate quantities of constituent elements of 5N purity in an argon arc furnace. Specimens in the form of rectangular parallelepipeds 1 mm × 1 mm × 20 mm, suitable

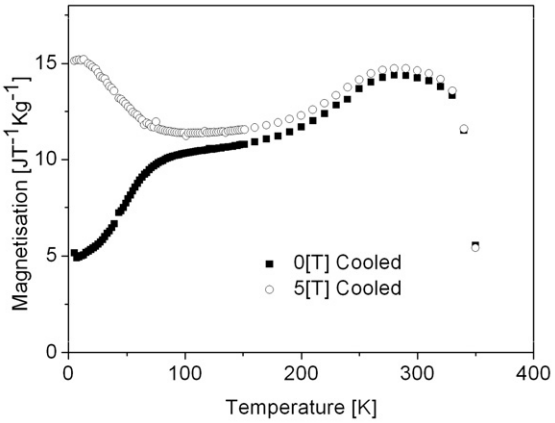

Figure 2. The magnetization of $Ni_2Mn_{1.48}Sb_{0.52}$ measured in a field of 0.05 T whilst heating from 5 K. The sample having first been cooled to 5 K in zero field (open symbols) or cooled in an applied field of 5 T (filled symbols).

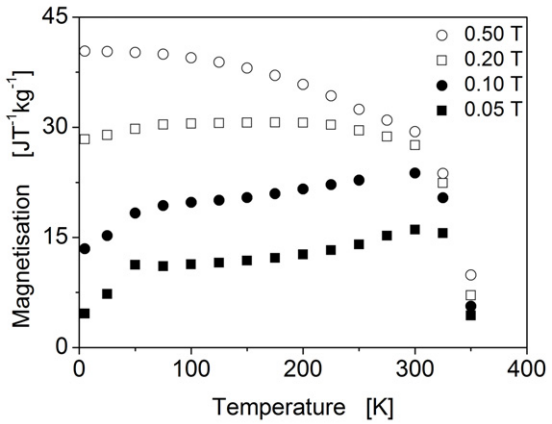

Figure 3. The magnetization of $Ni_2Mn_{1.48}Sb_{0.52}$ as a function of temperature measured in a series of different applied fields.

for resistivity measurements were spark eroded from the ingot. The remainder was readily powdered in a hardened steel pestle and mortar to a particle size less than 250 μm. The powder and resistivity specimens were then sealed in a quartz ampoule and annealed at 800 °C for 24 h before being water quenched. Subsequent x-ray diffraction measurements at room temperature showed that the sample was a single phase with the Heusler $L2_1$ structure (space group $Fm\bar{3}m$) and lattice parameter 5.958 Å in good agreement with that reported by Sutou *et al* [8].

A detailed structural determination was carried out using the high resolution neutron powder diffractometers D2b and D20 at the ILL in Grenoble. Since the coherent nuclear scattering amplitudes of the constituent elements, Ni (10.3 fm), Mn (−3.73 fm) and Sb (5.57 fm) are significantly different from one another, neutron diffraction is particularly appropriate. Furthermore neutrons are able to probe the bulk properties of specimens up to several cm^3. Using D2b and a neutron wavelength of 1.59 Å, diffraction patterns were recorded over the 2θ range 10°–150° in steps of 0.05°. The sample was cooled in an 'ILL orange cryostat' which provided stable temperatures between 5 and 310 K. Further measurements were made between 2 and 300 K with the sample in a cryomagnet enabling vertical fields of up to 5 T to be applied. The multi-detector on D20 enabled the integrated intensities of some of the weaker reflections to be measured as a function of temperature.

The bulk magnetic properties were investigated using a SQUID magnetometer in fields of up to 5.5 T and at temperatures between 5 and 350 K.

The variation in resistivity obtained whilst heating and cooling between 25 and 300 K was determined using a standard four probe technique. The specimen was thermally anchored to a sapphire plate attached to the cold stage of a closed cycle refrigerator. The apparatus was placed between the pole pieces of an electromagnet enabling fields of up to 0.2 T to be applied parallel to the long axis of the specimen.

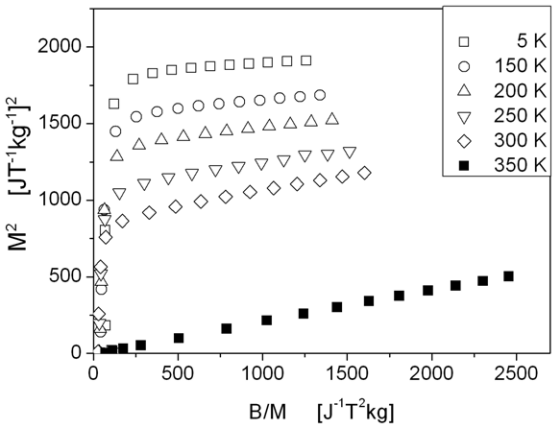

Figure 4. Magnetic isotherms for $Ni_2Mn_{1.48}Sb_{0.52}$ displayed in the form of Arrott plots (M^2 versus B/M). The 350 K isotherm passing through the origin defines the Curie temperature. The linearity of the isotherms confirms the magnetic homogeneity of the sample.

3. Results

3.1. Magnetization measurements

The magnetization in a field of 0.05 T observed whilst heating from 5 to 350 K is shown in figure 2, for a sample first cooled in zero field and subsequently in a field of 5 T. From these measurements two anomalies could be identified, one around 100 K and the other at approximately at 300 K. As the field is increased the anomalies become less pronounced as shown in figure 3 and in a field of 0.5 T the magnetization approaches that expected for an isotropic ferromagnet. Magnetic isotherms measured at 25 K intervals in fields up to 5.5 T are presented in the form of Arrott plots (M^2 versus B/M) in figure 4. The isotherm passing through the origin fixes the Curie temperature as 350 K. Extrapolation of the high field portion of the isotherms gives the thermal variation of the spontaneous magnetization shown in figure 5 and in reduced form in figure 6. The spontaneous magnetization of 42.54 J T^{-1} kg^{-1} at 5 K, corresponds to a moment of ≈2.0 μ_B/f.u..

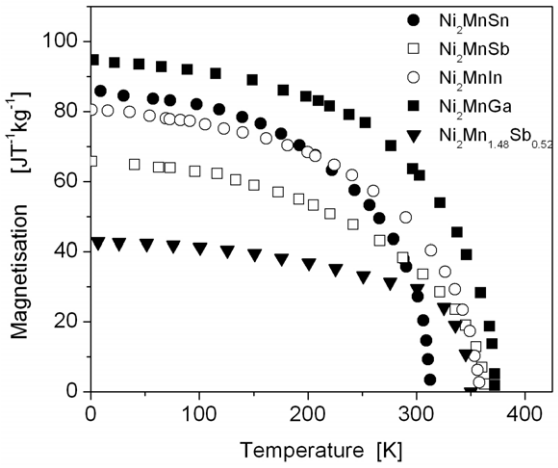

Figure 5. The thermal variation of the spontaneous magnetization of $Ni_2Mn_{1.48}Sb_{0.52}$ compared with that of related Ni_2MnZ Heusler alloys [19].

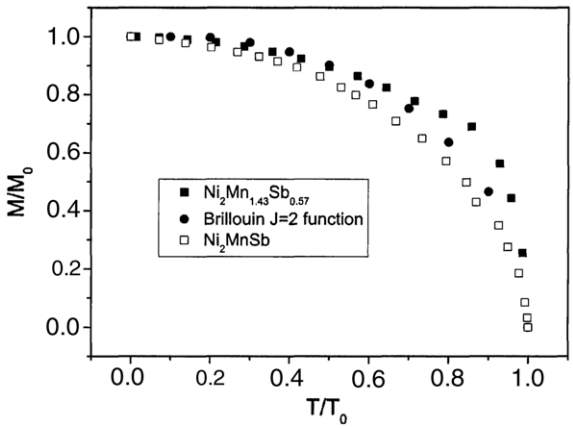

Figure 6. The reduced magnetization of $Ni_2Mn_{1.48}Sb_{0.52}$ plotted as a function of reduced temperature together with that for Ni_2MnSb. For comparison the Brillouin function for $J = 2$ is also plotted.

Table 1. Values of the bulk magnetic properties of $Ni_2Mn_{1.48}Sb_{0.52}$.

Curie temperature	T_C	350(5)	K
Spontaneous magnetization at 5 K	$M_{0,5}$	42.54(5)	J T^{-1} kg^{-1}
Spontaneous magnetization at 300 K	$M_{0,300}$	29.43(4)	J T^{-1} kg^{-1}
Magnetic moment per formula unit at 5 K	$\mu_{0,5}$	2.01(5)	μ_B
Magnetic moment per formula unit at 300 K	$\mu_{0,300}$	1.38(5)	μ_B
Temperature of resistivity minimum		262(5)	K
Temperature of minimum $\delta\rho/\delta T$		211(5)	K

A summary of the bulk magnetic properties of $Ni_2Mn_{1.48}Sb_{0.52}$ is given in table 1 and the magnetization of this and related Ni_2MnZ alloys is shown in figures 5 and 6.

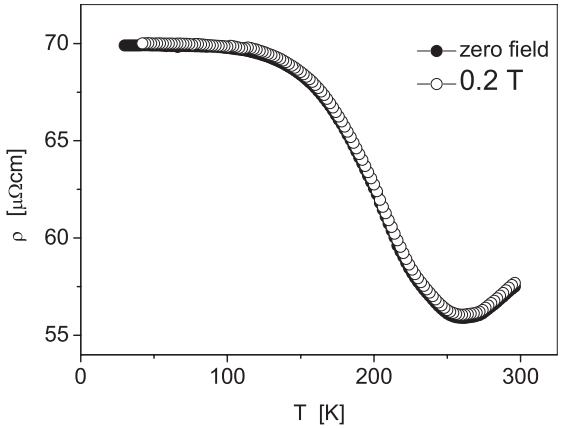

Figure 7. The thermal variation of the resistivity of $Ni_2Mn_{1.48}Sb_{0.52}$ obtained whilst cooling from 350 K in zero field and with an applied field of 0.2 T applied along the current direction.

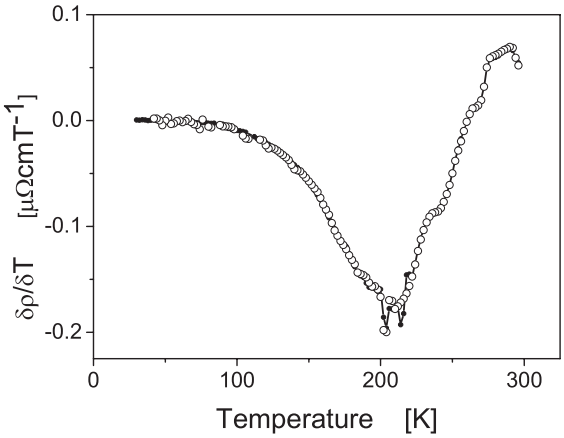

Figure 8. The thermal derivatives of both sets of resistivity data shown in figure 7.

3.2. Resistivity measurements

The variation in resistivity observed whilst heating and cooling between 25 and 300 K in zero field is shown in figure 7. Although the absolute change in resistivity is small the temperature dependence is similar to that observed in related systems that undergo a martensitic phase transition. There is a slight hysteresis ≈3 K in the position of the minimum between the heating and cooling cycles as expected for a structural phase transition, the mean value being 262 K. The thermal derivative of the resistivity which is similar for both cycles is shown for the cooling cycles in both zero and 0.2 T fields in figure 8. The features which can be seen include a minimum around 210 K, and discontinuities at ≈235, ≈266 and ≈277 K as shown in figures 7 and 8. Application of a field of 0.2 T did not produce any apparent change in resistivity in contrast to the change in magnetization produced by the same field.

3.3. Neutron measurements

The neutron diffraction pattern obtained below the Curie temperature (T_C = 350 K) at 310 K and shown in figure 9

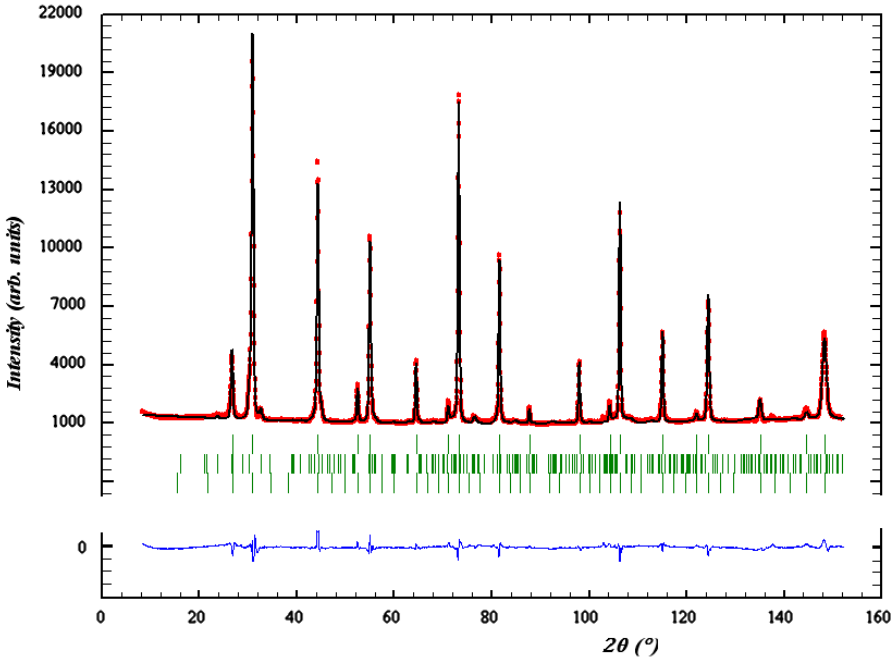

Figure 9. The observed (dots) and calculated (solid line) neutron powder diffraction patterns of $Ni_2Mn_{1.48}Sb_{0.52}$ at 310 K. The lower curve shows the difference between the observed and calculated patterns. The upper vertical tick marks give the position of the nuclear Bragg peaks for the Heusler $L2_1$ phase. Those below correspond to the position of the orthorhombic peaks and possible magnetic reflections.

Table 2. Parameters obtained from refinements of the neutron diffraction patterns from $Ni_2Mn_{1.48}Sb_{0.52}$.

Temperature (K)	310		5		
Structure/space group	$L2_1$ cubic $Fm\bar{3}m$		Orthorhombic $Pmma$		
Cell	$a = 5.958(2)$ Å		$a = 8.553(2)$ $b = 5.590(2)$ $c = 4.342(2)$ Å		
Cell volume (Å^3)	211.50		206.16		
Atom	Site	μ (μ_B)	Site	y	z
Ni	8(c) $\frac{1}{4}\frac{1}{4}\frac{1}{4}$		4(h) $0y\frac{1}{2}$	0.2571(14)	
			4(k) $\frac{1}{4}yz$	0.2325(10)	0.0903(5)
Mn	4(a) 000	1.57(12)	2(a) 000		
			2(f) $\frac{1}{4}\frac{1}{2}z$		0.5605(17)
0.48Mn + 0.52Sb	4(b) $\frac{1}{2}\frac{1}{2}\frac{1}{2}$	0.15(9)	2(b) $0\frac{1}{2}0$		
			2(e) $\frac{1}{4}0z$		0.4999(10)

contains 19 strong Bragg reflections all of which could be indexed using a fcc cell. The peaks were sharp, their widths being resolution limited providing further confirmation of the structural homogeneity of the sample. There were several additional small peaks which could be identified with a low temperature martensitic structure similar to that observed for $Ni_2Mn_{1.44}Sn_{0.56}$ which had an orthorhombic structure based on a two fold modulation $\mathbf{a}_{orth} = (\mathbf{a}_{cub} + \mathbf{b}_{cub})$; $\mathbf{b}_{orth} = \mathbf{c}_{cub}$; $\mathbf{c}_{orth} = (\mathbf{a}_{cub} - \mathbf{b}_{cub})$ and space group $Pmma$. Profile refinement of the high angle Bragg peaks confirmed that the specimen was highly ordered in the $L2_1$ structure. Since the coherent nuclear scattering amplitudes of the constituent elements are significantly different it was possible to determine the occupancies of each site which showed that the excess manganese atoms preferentially occupy vacant antimony (B) sites. At 310 K the specimen is still ferromagnetic and in Ni_2MnGa and other compounds in the Ni_2MnZ series [19] most of the magnetic moment is due to the manganese atoms and only a small amount ≈0.3 μ_B is carried by the nickel. Assuming this is also true for $Ni_2Mn_{1.48}Sb_{0.52}$, a magnetic moment with a Mn^{2+} form factor was introduced on both sites containing Mn in the Heusler phase and a fraction of remanent martensitic phase, was included in subsequent refinements of the whole pattern. Initially the magnitudes of the manganese moments on the two sites were constrained to be equal but a significantly improved fit was obtained by allowing them to differ. The relative orientation of the moments was also allowed to vary in the refinements. The best fit was found with almost zero moment on the 4b sites. The results are given in table 2 and the observed and calculated profiles are shown in figure 9 together with the difference pattern. The total moment due to Mn on both the A and B sites (1.42(10) μ_B) is in good agreement with the value of 1.36(3) μ_B obtained from magnetization measurements. A subsequent refinement

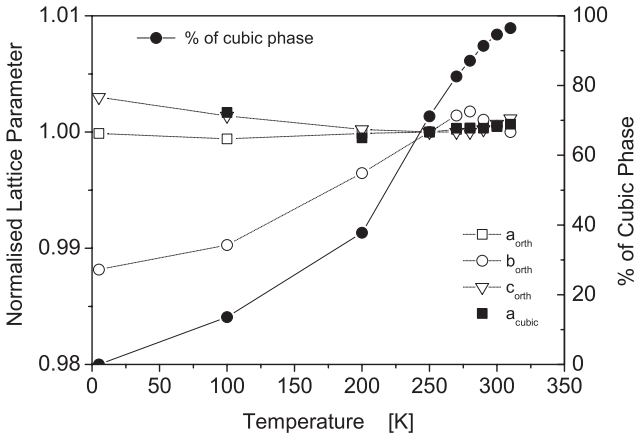

Figure 10. The percentage of cubic phase in $Ni_2Mn_{1.48}Sb_{0.52}$ together with the fractional variation of the cubic and orthorhombic lattice parameters, normalized to their values at 250 K, as a function of temperature. Lines joining equivalent points have been inserted as guides to the eye.

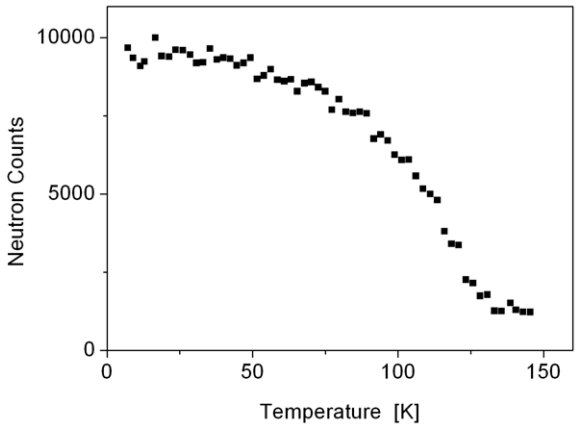

Figure 11. The thermal variation of the satellite reflection $(4/3, 2/3, 0)$ observed at $2\theta = 18°$.

in which the Ni atoms were also allowed to carry a moment did not improve the goodness of fit as indicated by a χ^2 test

$$\chi^2 = \sum[(I_{\rm obs} - I_{\rm calc})/\sigma I_{\rm obs}]^2/(N_{\rm obs} - N_{\rm par})$$

where $N_{\rm obs}$ is the number of observations and $N_{\rm par}$ is the number of parameters.

As the temperature was lowered from 310 K the intensity of the orthorhombic peaks increased whilst those of the cubic parent phase fell. The results of a series of refinements using data collected at temperatures between 310 and 5 K are summarized in figure 10. The diffraction pattern evolved continuously with decreasing temperature and the orthorhombic phase only became dominant at the lowest temperatures. Above 200 K the cubic austenite cell together with an orthorhombic martensite cell with space group $Pmma$ could account for all observed reflections and did not generate any which were not observed. The relationship between the atomic sites occupied in the $Fm\bar{3}m$ and $Pmma$ space groups is indicated table 2 and leads to five refinable position parameters for the orthorhombic phase. Comparison of the diffraction patterns obtained at 200 and 5 K revealed two very weak additional reflections in the low temperature data. The peaks occur at relatively low scattering angles of 18.0° and 36.09° with wavevectors of 1.229 $Å^{-1}$ and 2.433 $Å^{-1}$ respectively. The mean of these wavevectors, 1.831 $Å^{-1}$, coincides with the 210 nuclear Bragg position (1.837 $Å^{-1}$) and if the two are indexed as satellites of this reflection leads to a propagation vector $(2/3, 1/3, 0)$. The thermal variation of the intensity of the satellite at $2\theta = 18.0°$ measured using the multi-detector on D20 is shown in figure 11 and establishes the transition temperature of the modulated phase as 132(7) K. A series of scans made through the whole angular range at temperatures between 5 and 300 K and at fields up to 5 T did not show any significant change in the positions or intensities of either the main or the satellite peaks.

An initial refinement of the nuclear structure at 5 K was made using the high angle diffraction data ($2\theta > 60°$) and the orthorhombic cell with atom sites as given in table 2. The results of this refinement were used to simulate the diffraction pattern for the full angular range covered in the experiment. This simulation showed that only one peak in the pattern, that made up of the 210 and 011 reflections, contained significant magnetic scattering. Furthermore, apart from the two weak satellite reflections no additional reflections which might have purely magnetic origin were observed. In principle for an orthorhombic structure it is possible to determine the magnitude of the moment and its orientation with respect to the crystallographic axes. However the paucity of significant magnetic scattering and the more complex diffraction pattern makes such an analysis impracticable in the present case. The refinement of the 310 K data showed that the moments at the 4(b) site were small. Therefore in the initial refinement of the magnetic structure at 5 K, magnetic moments were only assigned to the 2(a) and 2(f) sites. A series of collinear and canted models with zero propagation vectors was tried. Although the magnetic contribution to the peaks was in general small, the absence of significant magnetic scattering in some of the low angle reflections, e.g. 100, places severe constraints on the moment direction. In all models considered the magnetic scattering in the 210 and 011 reflections arises from a ferromagnetic component. The three models which gave the best agreement with the observations are presented in table 3, The mean moment per cell can be seen to be very similar for all three models. In model 1 ferromagnetically aligned moments were constrained to be parallel to [100]; the fitted pattern is shown in figure 12 together with the difference between the calculated and observed profiles. Very similar fits were obtained for the other two models; in model 2 the moments were aligned parallel to [001] and in model 3 were constrained to the (010) plane. The magnetic contribution to the data was not sufficient to allow moment values to be refined for the Ni atoms or for the Mn atoms on the 2(b) and 2(e) sites.

4. Discussion

Measurements on a number of Heusler alloys have shown that a structural phase transition occurs if e/a based on the total electron number is close to 7.8. For $Ni_2Mn_{1.48}Sb_{0.52}$ the ratio

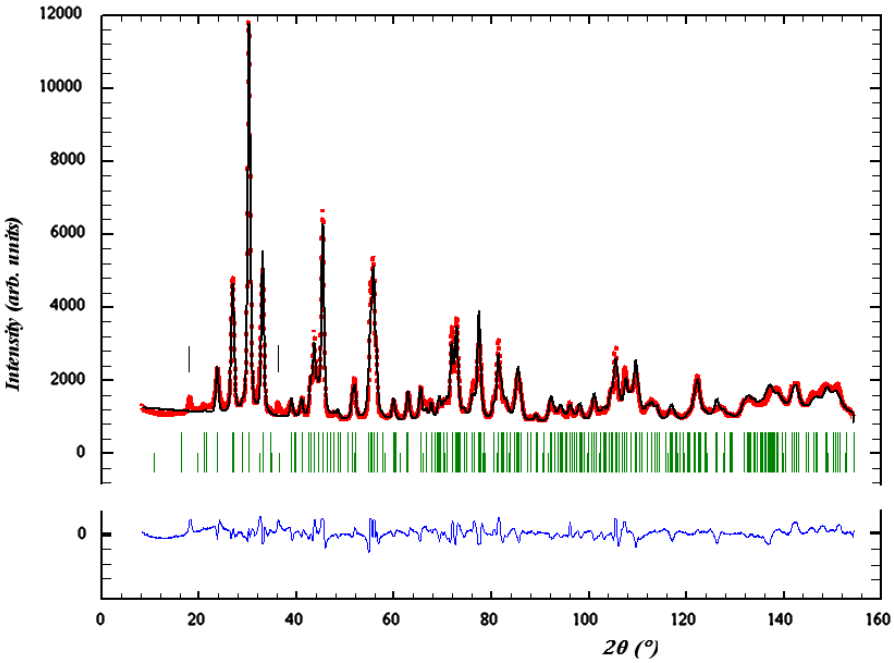

Figure 12. The observed (dots) and calculated (solid line) neutron powder diffraction patterns of $Ni_2Mn_{1.48}Sb_{0.52}$ at 5 K. The position of the satellite reflections are indicated by the two vertical lines above the pattern. The lower curve shows the difference between the observed and calculated patterns. The upper vertical tick marks give the position of the nuclear Bragg peaks for the orthorhombic phase and those below indicate possible magnetic reflections.

Table 3. Parameters obtained in refinements of the magnetic structure of $Ni_2Mn_{1.48}Sb_{0.52}$ using the three models described in the text.

Model		1	2	3	
Site		M_x (μ_B)	M_z (μ_B)	M_x (μ_B)	M_z (μ_B)
	000			0.04	3.702
2(a)		3.99	4.02		
	$\frac{1}{2}$ 00			−0.04	3.702
	$\frac{1}{4}\frac{1}{2}z$			1.458	3.548
2(f)		3.70	3.60		
	$\frac{3}{4}\frac{1}{2}z$			−1.458	3.548
R_m		6.23	6.7	7.2	

is 7.47. Neutron diffraction measurements on four Ni–Mn–Z alloys show that the period of modulation of the martensite phase is odd when Z is a group 3b element Ga ($n = 7$) or In ($n = 3$) [11, 14] whereas those containing Sn or Sb have an even periodicity; $n = 2$ as for both $Ni_2Mn_{1.44}Sn_{0.56}$ [18] and $Ni_2Mn_{1.48}Sb_{0.52}$. However measurements on a series of quaternary alloys indicate that electron concentration is not the dominant factor determining T_M [20, 21]. The neutron diffraction measurements indicate that the structural phase transition which occurs in $Ni_2Mn_{1.48}Sb_{0.52}$ is essentially continuous with the martensitic phase only being fully established below 50 K. It is for this reason that the low field magnetization does not exhibit the abrupt drop generally observed at T_M [4] as a result of the lower crystal symmetry and associated increase in the magnetic anisotropy. In contrast the resistivity shows a distinct anomaly at 262 K, similar to that observed in both paramagnetic and ferromagnetic related systems at T_M [22–24]. If the increase in resistivity observed below 262 K were due to an energy gap in the electronic structure, the thermal variation would imply a gap of ≈100 K. However band structure calculations for a number of shape memory alloys [25, 26] reveal nesting features for parts of the Fermi surface at wavevectors characterizing the modulations observed in the martensitic structures. Gaps which open in the electronic structure would then reduce the carrier density producing an increase in the resistivity as observed on cooling below ≈262 K. However the transition begins at a relatively high temperature ≈300 K at which the resistivity should be dominated by lattice effects and takes place over a wide temperature range; the system is not in thermodynamic equilibrium and to account for the overall variation in resistivity the influence of the microstructure needs to be considered. Examination of the thermal variation of the resistivity reveals the presence of a series of small discontinuities which can be seen more clearly in its thermal derivative. The discontinuities are not affected by the application of small magnetic fields applied parallel to the direction of the current and may be associated with thermally activated partial dislocations. The atomic shifts perpendicular to the modulation axis obtained from the structural refinement of the martensitic phase are shown schematically in figure 13. They are rather different from the periodic displacements expected for the ideal $2\bar{2}$ martensite shown in figure 1. In particular the atoms on the Heusler 4b sites (Sb, Mn) do not shift at all. As with other related martensites atomic shifts occur along both the y and z axes indicating the modulation is not simply planar.

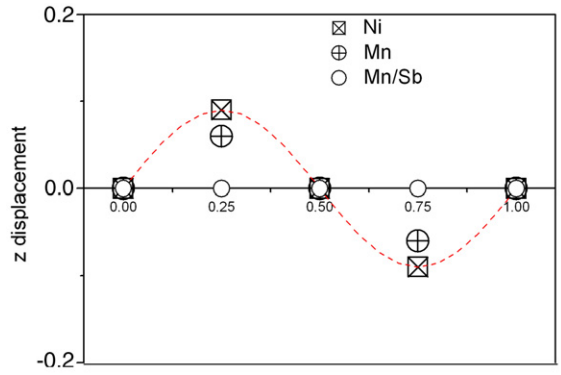

Figure 13. The atomic displacements perpendicular to the axis of modulation obtained from the refinement of the 5 K neutron diffraction data.

$Ni_2Mn_{1.48}Sb_{0.52}$ orders ferromagnetically below 350 K, at which temperature the sample is predominantly in the cubic austenite phase. On cooling from 350 to −5 K the spontaneous magnetization has the variation expected for an isotropic ferromagnet. The reduced spontaneous magnetization, shown in figure 6, follows the variation of the Brillouin function for $J = 2$ except for the region around 280 K where the structural phase transition begins to accelerate. The magnetization of the stoichiometric compound, which does not have a structural phase transition, is also plotted in figure 4, and falls slightly faster than the Brillouin function. However the ground state moment per $Ni_2Mn_{1.48}Sb_{0.52}$ formula unit is only 2 μ_B, considerably lower than the 3.5 μ_B found for Ni_2MnSb which is itself lower than that of other alloys in the Ni_2MnZ series with the $L2_1$ structure (Z = Ga, In and Sn) [19]. Ni_2MnAl which has the B2 structure orders antiferromagnetically below 300 K [27]. It is well established that the magnetic properties of Heusler alloys X_2MnZ are strongly influenced by the groups to which the X or Z atoms belong. In alloys in which the Z atom is a group 3b element such as Al or In disorder tends to occur between the Al and Mn sites and there is propensity for antiferromagnetic order. On the other hand alloys containing group 4 or 5b elements are normally highly ordered in the $L2_1$ structure and are ferromagnetic. The present measurements on $Ni_2Mn_{1.48}Sb_{0.52}$ at 310 K show that the Mn moment on the 4a site is 1.44 μ_B which is close to that observed for other related Heusler alloys at 0.89 times T_c. Extrapolation to 5 K using the $J = 2$ Brillouin function gives 3.5 μ_B. On the other hand the excess Mn atoms occupying the 4b sites have nearly zero moment although in stoichiometric Heusler alloys the Mn moment is essentially independent of the degree of $L2_1$–B2 atomic order. However if a second atom carries a moment, usually on the 8c site, its value is smaller than in its elemental state e.g. Ni ≈0.3 μ_B, Co ≈0.5–0.75 μ_B [19]. In $Ni_2Mn_{1.48}Sb_{0.52}$ the Mn atoms in the 4b sites, unlike those in the 4a sites, have 6 Mn neighbours at a distance of $a/2 \approx 2.98$ Å. The increased d–d overlap may give rise to the observed loss of moment.

No evidence has yet been found for a field induced transition to a state of higher magnetization in the martensite phase of $Ni_2Mn_{1.48}Sb_{0.52}$ such as that as observed in $Ni_2Mn_{1.44}Sn_{0.56}$. Further magnetization measurements in applied fields above 5.5 T are required to clarify this point.

Departure from isotropic magnetic behaviour at lower temperatures is evident from the low field magnetization below 300 K. As shown in figure 3 the low field magnetization of a zero field cooled sample becomes smaller below ≈100 K whereas that of a sample cooled in a field of 5 T increases. Such behaviour is usually observed in frustrated systems as a result of competing ferro and antiferromagnetic interactions. The neutron diffraction measurements reveal the presence of satellite reflections in the same temperature range although similar measurements in the austenite phases of Ni_2MnGa, $Ni_2Mn_{1.44}Sn_{0.56}$ and $Ni_2Mn_{1.48}In_{0.52}$ have not shown the presence of an incommensurate phase. Magneto-elastically driven incommensurate structures have been reported in related Co–Ni–Al and Co–Ni–Ga systems based on tweed patterns observed in electron microscopy [28]. However neutron diffraction measurements did not reveal any indication of incommensurate structures [29]. The present neutron diffraction study shows that in $Ni_2Mn_{1.48}Sb_{0.52}$ an incommensurate magnetic modulation, which is an intrinsic property of the ferromagnetic martensite, appears below 132 K: it has a temperature independent wavevector 2/3, 1/3, 0.

References

[1] Ullakko K, Haung J K, Kanter C, Korkorin V V and O'Handley R C 1996 *Appl. Phys. Lett.* **69** 1966
[2] Nishiyama H 1978 *Martensitic Transformation* (New York: Academic)
[3] Otsuka K and Wayman C M 1998 *Shape Memory Materials* (Cambridge: Cambridge University Press)
[4] Webster P J, Ziebeck K R A, Town S L and Peak M S 1984 *Phil. Mag.* **49** 295
[5] Fröhlich K, Dennis D, Kanomata T, Matsumoto M, Neumann K-U and Ziebeck K R A 2005 *Int. J. Appl. Electromag. Mech.* **21** 159
[6] Krenke T, Acet M, Wassermann E F, Moya X, Manosa L and Planes A 2006 *Phys. Rev.* **73** 174413
[7] Ito W, Imano Y, Kainuma R, Satou Y, Oikawa K and Ishida K 2007 *Metall. Mater. Trans.* A **37** 759
[8] Sutou Y, Imano Y, Koeda N, Omari T, Kainuma T, Ishida K and Oikawa K 2004 *Appl. Phys. Lett.* **85** 4358
[9] Oikawa K, Ito W, Imano Y, Sutou Y, Kainuma R, Ishida K, Okamoto S, Kitakami O and Kanomata T 2006 *Appl. Phys. Lett.* **88** 122507
[10] Koyama K, Watanabe K, Kanomata T, Kainuma R, Oikawa R and Ishida K 2006 *Appl. Phys. Lett.* **88** 132505
[11] Gandy A P 2007 *PhD Thesis* Department of Physics, Loughborough University
[12] Kahn M, Dubenko I, Stadler S and Ali N 2008 *J. Phys.: Condens. Matter* **20** 235204
[13] Du J, Zheng Q, Ren W J, Feng W J, Lui X G and Zhang Z D 2007 *J. Phys. D: Appl. Phys.* **40** 5523
[14] Brown P J, Crangle J, Kanomata T, Matsumoto M, Ouladdiaf B, Neumann K-U and Ziebeck K R A 2002 *J. Phys.: Condens. Matter* **14** 10159
[15] Neumann K-U, Kanomata T, Ouladdiaf B and Ziebeck K R A 2002 *J. Phys.: Condens. Matter* **14** 1371
[16] Brown P J, Gandy A P, Ishida K, Kainuma R, Kanomata T, Neumann K-U, Oikawa K, Ouladdiaf B and Ziebeck K R A 2006 *J. Phys.: Condens. Matter* **18** 2249

[17] Brown P J, Dennis B, Crangle B, Kanomata T, Matsumoto M, Neumann K-U, Justham L M and Ziebeck K R A 2004 *J. Phys.: Condens. Matter* **16** 65
[18] Brown P J, Gandy A P, Ishida K, Kainuma R, Kanomata T, Neumann K-U, Oikawa K and Ziebeck K R A 2006 *J. Phys.: Condens. Matter* **19** 016201
[19] Webster P J and Ziebeck K R A 1988 *Landolt Boernstein Neue Serie* vol VIII/19c (Berlin: Springer) section 1.5.5
[20] Anders P 2003 *M. Phil.* Department of Physics, Loughborough University
[21] Marshai K El 2008 *M. Phil.* Department of Physics, Loughborough University
[22] Watanabe Y, Mori Y and Sato A 1993 *J. Mater. Sci.* **28** 1509
[23] Khovalio V V, Oikawa K, Wedel C and Takagi K 2004 *J. Phys.: Condens. Matter* **16** 1951
[24] Kuo Y K, Sivakumar K M, Chen H C, Su J H and Lue C S 2005 *Phys. Rev.* B **72** 054116
[25] Zhao G L and Harmon B N 1992 *Phys. Rev.* B **45** 2818
[26] McDonald R D, Singleton J, Goddard P, Drymiotis F, Harrison N, Harima H, Suzuki M-T, Saxena A, Darling T, Migliori A, Smith J L and Lashley J C 2005 *J. Phys.: Condens. Matter* **17** L69
[27] Ziebeck K R A and Webster P J 1975 *J. Phys. F: Met. Phys.* **5** 1756
[28] Saxena A, Castan T, Planes A, Porta M, Kishi Y, Lograsso T A, Viehland D, Wuttig M and Graef D E 2004 *Phys. Rev. Lett.* **92** 197203
[29] Brown P J, Ishida K, Kainuma R, Kanomata T, Matsumoto M, Neumann K-U, Oikawa K, Ouladdiaf B and Ziebeck K R A 2005 *J. Phys.: Condens. Matter* **17** 1301